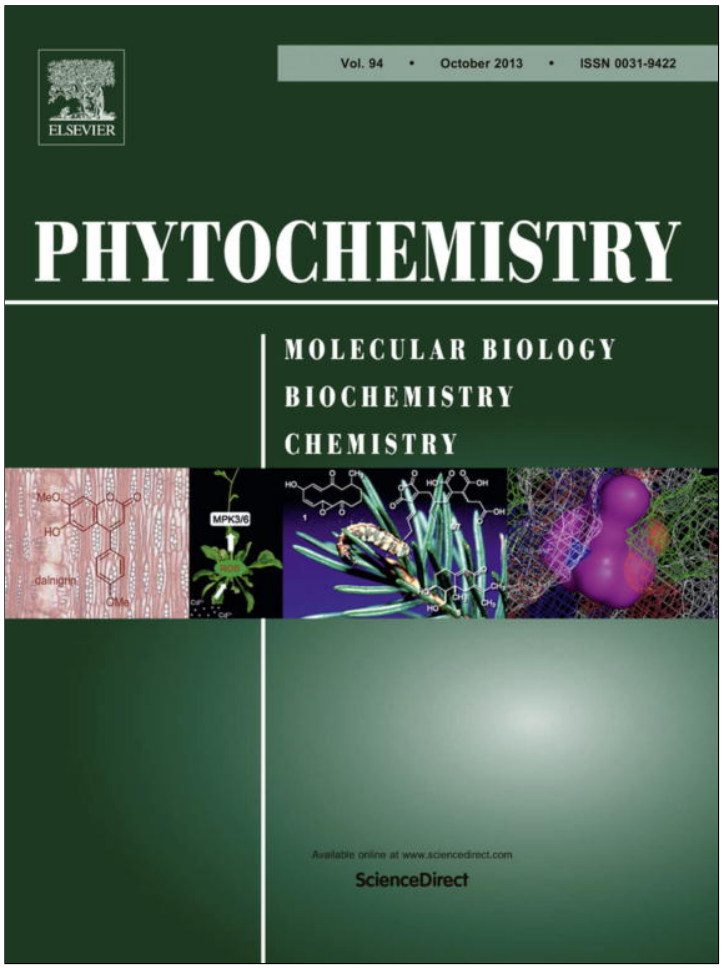

Phytochemistry 94 (2013) 45–52

Contents lists available at SciVerse ScienceDirect

Phytochemistry

journal homepage: www.elsevier.com/locate/phytochem

Abolishing activity against ascorbate in a cytosolic ascorbate peroxidase from switchgrass

Frank A. Kovacs [a,*], Gautam Sarath [b], Kyle Woodworth [a], Paul Twigg [c], Christian M. Tobias [d]

[a] Department of Chemistry, University of Nebraska at Kearney, Kearney, NE 68849, United States
[b] Grain, Forage and Bioenergy Research Unit, USDA-ARS, Lincoln, NE 68583-0937, United States
[c] Department of Biology, University of Nebraska at Kearney, Kearney, NE 68849, United States
[d] Genomics and Gene Discovery Research Unit, USDA-ARS, Albany, CA 94710, United States

ARTICLE INFO

Article history:
Received 25 January 2013
Received in revised form 8 May 2013
Available online 26 June 2013

Keywords:
Ascorbate
Peroxidase
Panicum virgatum
Poaceae
Mutant
ABTS

ABSTRACT

Switchgrass (*Panicum virgatum* L.) is being developed as a bioenergy species. Recently an early version of its genome has been released permitting a route to the cloning and analysis of key proteins. Ascorbate peroxidases (APx) are an important part of the antioxidant defense system of plant cells and present a well studied model to understand structure–function relationships. Analysis of the genome indicates that switchgrass encodes several cytosolic ascorbate peroxidases with apparent varying levels of tissue expression. A major cytosolic ascorbate peroxidase was thus selected for further studies. This gene was cloned and expressed in *Escherichia coli* cells to obtain purified active protein. Full heme incorporation of the enzyme was achieved utilizing slow growth and supplementing the media with 5-aminolevulinic acid. The enzyme was observed to be monomeric in solution via size exclusion chromatography. Activity toward ascorbate was observed that was non-Michaelis–Menten in nature. A site-directed mutant, R172S, was made in an attempt to differentiate activity against ascorbate versus other substrates. The R172S protein exhibited negligible ascorbate peroxidase activity, but showed near wild type activity toward other aromatic substrates.

1. Introduction

Cytosolic ascorbate peroxidase (APx) catalyzes the reduction of H_2O_2 utilizing small organic substrates as electron donors with the physiological substrate being ascorbate (AsA) as shown below (Eq. (1)).

$$H_2O_2 \xrightarrow{APX} 2H_2O + 2MDAsA \quad (1)$$

In plants, the monodehydroascorbate radical (MDAsA) is converted back to AsA by MDAsA reductase or in the absence of reductase, the 2 MDAsAs can disproportionate to AsA and dehydroascorbic acid (DAsA) (Chen et al., 2003; Shigeoka et al., 2002). The catalytic mechanism of ascorbate oxidation by APx has been well studied and is generally represented as shown in Eqs. (2)–(4), where APx first reacts with H_2O_2 and becomes Compound I, the fully oxidized form of APx. Compound I is converted back to APx via two one-electron transfers from an electron donating substrate (HS).

$$APX + H_2O_2 \rightarrow \text{Compound I} + H_2O \quad (2)$$

$$\text{Compound I} + HS \rightarrow \text{Compound II} + S^{\cdot} \quad (3)$$

$$\text{Compound II} + HS \rightarrow APX + S^{\cdot} + H_2O \quad (4)$$

There are many excellent reviews dealing with APx (Dunford, 1999; Raven, 2003; Raven et al., 2004), and only a brief review is provided here. Ascorbate-dependent peroxidases from spinach and pea were first described in 1979 (Groden and Beck, 1979; Kelly and Latzko, 1979) and are key proteins protecting cellular health in plants by scavenging peroxides generated during photosynthesis and cellular metabolism (Alvarez and Lamb, 1997; Bowler et al., 1992; Ishikawa and Shigeoka, 2008; Noctor and Foyer, 1998). They have been investigated at the structural and functional level because unlike cytochrome *c* peroxidase (CcP), one of the best known and characterized peroxidases, they have the more typical Compound I intermediate with a porphyrin-based radical and they utilize small molecule substrates as electron donors (Raven, 2003). Ascorbate-dependent peroxidases are essentially defined by having high specificity to ascorbate, which has a clear physiological role as an electron source for detoxifying cells of H_2O_2. However many of these enzymes also have significant activity toward other aromatic electron donors, which usually do not have clear physiological roles. For the most part, these ascorbate-dependent peroxidases have higher activity toward ascorbate than other substrates.

* Corresponding author. Address: Nebraska at Kearney, 4201 11th Ave., NE 68849, United States. Tel.: +1 308 865 8483; fax: +1 308 865 8399.
E-mail addresses: kovacsfa@unk.edu, kovacsfa1@gmail.com (F.A. Kovacs).

0031-9422/$ - see front matter © 2013 Elsevier Ltd. All rights reserved.
http://dx.doi.org/10.1016/j.phytochem.2013.05.016

A

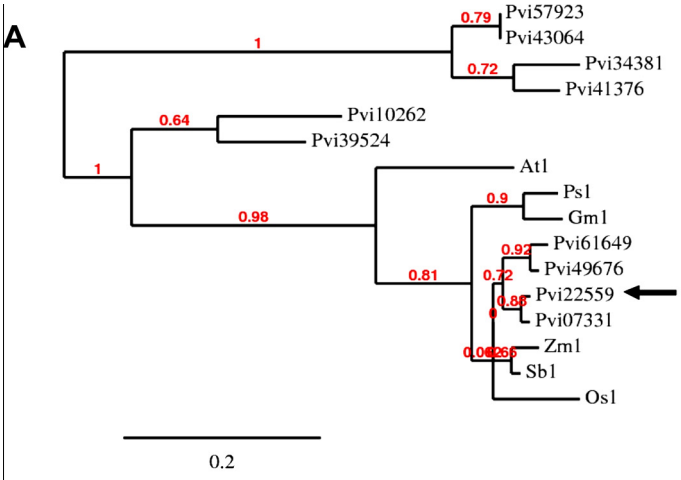

B

Database id	No. of ESTs	Cultivar, tissues and developmental stage	PviAPx1 Normalized
SRX057826	1,037,727	Alamo Root and Crown, reproductive stage	134.04
SRX057824	801,627	Alamo Shoot, unknown stage	70.48
SRX026153	240,166	Summer Whole Root, reproductive stage	34.98
SRX026148	211,124	Summer Shoot and crown, three weeks after trasplanting of in vitro plantlets	33.16
Sum_072010_Cr	317,557	Summer Crown, Anthesis	31.18
SRX057829	1,113,868	Alamo Root, reproductive-elongation stage	31.06
Sum_PreKill	930,114	Summer Crown, PreKilling Frost (Aug)	30.96
SRX026150	187,893	Summer Root, late internode elongation stage	29.27
SRX057832	2,310,834	Alamo Drought Stress Root, Stem Elongation Stage	27.78
SRX057831	1,317,713	Alamo Root, Leaf Developmental Stage	22.31
Sum_060711_StemLeaf	380,281	Summer Stem and Leaf, Vegetative	21.83
SRX057825	731,956	Alamo Root, unknown stage	21.45
Sum_062310_Cr	379,264	Summer Crown, Vegetative	19.25
Sum_051011_Cr	445,432	Summer Crown, Green-Up	18.41
SRX057827	557,570	Alamo Shoot, reproductive stage	14.71
SRX057833	378,037	Alamo Drought Stress Shoot, Stem Elongation Stage	14.28
SRX026155	240,696	Summer Flower-Seed, reproductive stage	14.13
SRX026146	284,325	Alamo-Vascular Bundle (Laser-capture microdissection, LCM)	14.07
SRX026151	228,101	Summer Whole Shoot excluding Flower, reproductive stage	13.59
Kanlow_PreKill	266,441	Kanlow Crown, PreKilling Frost (Aug)	12.01
SRX026145	271,307	Alamo-Whole Tissue (LCM)	10.69
SRX057834	1,143,746	Alamo Flower and Seeds, Reproductive Stage	10.67
SRX026147	265,190	Summer Root, three weeks after trasplanting of in vitro plantlets	9.05
SRX119550	245,995	Cimarron Tillers, Unknown Stage	6.50
SRX057828	1,407,916	Alamo Shoot, reproductive-elongation stage	5.40
SRX057830	1,298,485	Alamo Shoot or Leaf	4.24
Sum_PostKill	389,555	Summer Crown, Post Killing Frost (Nov)	0.51
SRX026149	210,071	Summer Shoot, late internode elongation stage	0.48
SRX119551	269,422	Cimarron Flowers, Unknown Stage	0.37
SRX119470	270,547	Cimarron Germinating Seedlings	0.37
Kanlow_PostKill	421,264	Kanlow Crown, Post Killing Frost (Nov)	0.24
SRX119552	193,426	Cimarron dormant seeds, unknown stage	0.00

Fig. 1. Phylogenetic relationships of PviAPx1 (A) (Pvi22559; arrow). Other switchgrass Apx sequences are identified by Pvi. The full database entry will read, for example as Pavirv00022559 m etc. Other cytosolic APx sequences used for this analysis are: At1 = *Arabidopsis thaliana*; Ps1 = *Pisum sativum*; Gm1 = *Glycine max*; Zm1 = *Zea mays*; Sb1 = *Sorghum bicolor*; Os1 = *Oryza sativa*.Relative expression of PviAPx1 in switchgrass tissues (B).

Crystal structures of APxs have been used to identify two different substrate binding sites, one for ascorbate (PDB ID: 1OAF) (Sharp et al., 2003) and one for aromatic substrates (PDB IDs: 1VOH, complexed with salicyhydroxamic acid and 2VCS, complexed with isoniazid)(Metcalfe et al., 2008; Sharp et al., 2004). This would strongly indicate that the substrate specificity for the other aromatic compounds comes from a different binding site than that of ascorbate.

In 1995, the first crystal structure of APx was determined for recombinant pea cytosolic APx (PDB ID: 1APX) (Patterson and Poulos, 1995). This structure showed a dimeric enzyme held together noncovalently by ionic interactions. The structure was remarkably similar to that of CcP, especially in the heme active site where the same hydrogen bonds exist between key conserved amino acids that are known to be essential for function. One striking difference was the discovery of a cation (K^+) binding site that has been observed to influence the ligation of the distal histidine to the heme iron (Cheek et al., 1999). In 2003, another set of structures were determined for recombinant soybean cytosolic APx that included a structure of the APx-ascorbate complex (PDB ID: 1OAF) (Sharp et al., 2003). This structure positively identified the γ-edge of the heme as the primary location of ascorbate binding and paved the way to better understanding the electron transfer mechanism for the enzyme. Presently, there are almost 30 APx structures in the protein structural database (http://www.rscb.org) that are predominantly mutant structures for cytosolic APx.

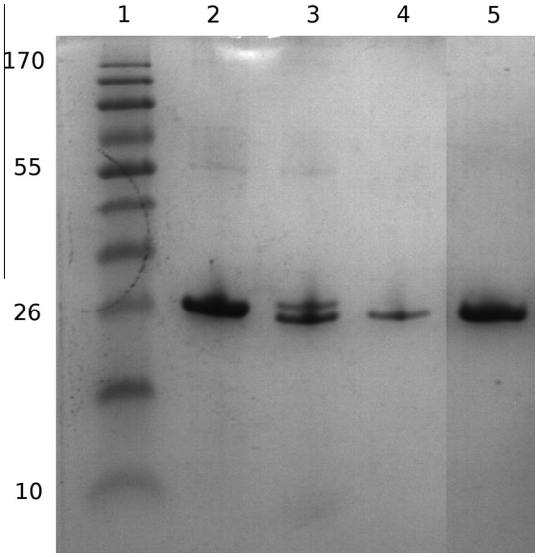

Fig. 2. SDS–PAGE of Ni–NTA purified rPviAPx before and after thrombin cleavage of 6X-His tag. (1) Marker. (2) Desalted Ni–NTA purified before cleavage. (3) Thrombin cleavage reaction. (4) Purified protein collected by running cleavage reaction over Ni–NTA column. (5) 5× volume of lane 4 sample demonstrating relative purity.

APx has proven to be a useful platform for protein engineering studies of peroxidases (Cheek et al., 1999). Most recently, APx has been engineered as a reporter for electron microscopy that can be used for imaging of mammalian organelles (Martell et al., 2012).

In the work reported here, a major cytosolic APx from switchgrass (rPviAPx) was cloned, expressed and its initial characterization performed; interestingly, switchgrass has been targeted as a biofuel crop (Sarath et al., 2008). Additionally, homology modeling was also performed using crystal structural models of APx and site-directed mutagenesis on a key amino acid found in the ascorbate binding site, Arg 172 (R172). This residue has been previously identified as essential for ascorbate binding such that even conservative size and charge changes like R172K dramatically lower activity toward ascorbate (Macdonald et al., 2006). This residue was thus mutated to a serine (R172S) both to validate our homology model and test the effect of placing a much smaller polar amino acid (previously untested mutation) in a position between the ascorbate and predicted aromatic substrate binding sites.

2. Results and discussion

2.1. Sequence analysis

Using the early release of the switchgrass genome (Draft0.0, http://www.phytozome.org), the fully sequenced PviAPx gene was found to be identical to a cytosolic ascorbate peroxidase encoded by the gene Pavirv00022559m.g. A BLAST (Altschul et al., 1990) analysis of this sequence showed that there were at least 12 other closely related sequences in the switchgrass genome (e-value threshold of 4.2×10^{-91} or lower), leading us to speculate that there were a total of six APx genes each in the A and B genomes. APx can be nominally assigned to three different clades, comprising the chloroplastic, peroxisomal and cytosolic proteins (Teixeira et al., 2004). Similarly, available switchgrass APx protein sequences appeared to be clearly distinguishable into three clades (Fig. 1A). Comparison of the switchgrass sequences annotated as cytosolic APxs with six other cytosolic APx sequences obtained from the NCBI database was carried out, namely: *Zea mays* APx1 (NP_001152249.1); *Sorghum bicolor* APx1 (XP_002468053.1); *Oryza sativa* APx1 (NP_001049769.1), *Pisum sativum* APx01(AAA33645), *Glycine max* APx1 (NP_001237785.1), and *Arabidopsis thaliana* APx1 (NP_172267.1). This was essential to validate the identification of the switchgrass cDNA clone as a cytosolic APx, as it is closely related to the other monocot cytosolic APx, and is also relatively closely related to the dicot sequences used for these analysis. To further confirm that this specific switchgrass APx is expressed in cells, a bioinformatic analysis was performed of relative transcript abundances in a number of different tissues (Fig. 1B). rPviAPx is abundantly expressed in most tissues obtained from several different switchgrass cultivars, suggesting that this enzyme is an important part of the switchgrass cellular antioxidant defense.

When compared to other recombinant APxs of solved crystal structures, it has a very high sequence similarity to both recombinant pea (rPsAPx01) and soybean (rGmAPx1) with 82% identity/90% positive and 85% identity/90% positive, respectively. This level of identity indicates that both of these enzymes would be useful for developing a homology structural model of rPviAPx.

2.2. rPviAPx characterization

Expression of holo rPvAPx depends on the simultaneous production of protein and heme by the bacteria. This requirement was met by supplying the bacteria with the heme precursor, 5-amino levulinic acid (5-ALA) and "slow growing" the cultures prior to induction with lower temperature (31 °C) and gentler shaking (150 rpm). The cultures at this point generally had a reddish color when compared to cultures without the 5-ALA, which was interpreted as production of excess heme. Once protein expression was induced with isopropyl β-D-1-thiogalactopyranoside (IPTG), the newly expressed APx was able to fully incorporate heme due to this excess. Growing the protein this way allowed for a reproducible expression of holo rPviAPx for both WT and mutant. Protein purity was then characterized both by Rz (~2.25) and SDS–PAGE. In gels of the proteins, routine purification to a single band at ~26 kDa was achieved. Occasionally, it was observed that a faint impurity at about 54 kDa was present, which is possibly some kind of covalently linked dimer of the protein. Fig. 2 shows a typical SDS–PAGE of rPviAPx before and after thrombin cleavage. Lanes

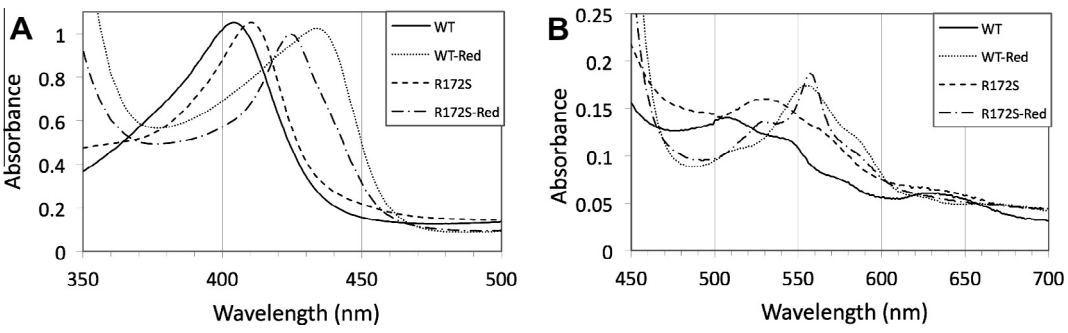

Fig. 3. Spectra of reduced WT and mutant rPviAPx.

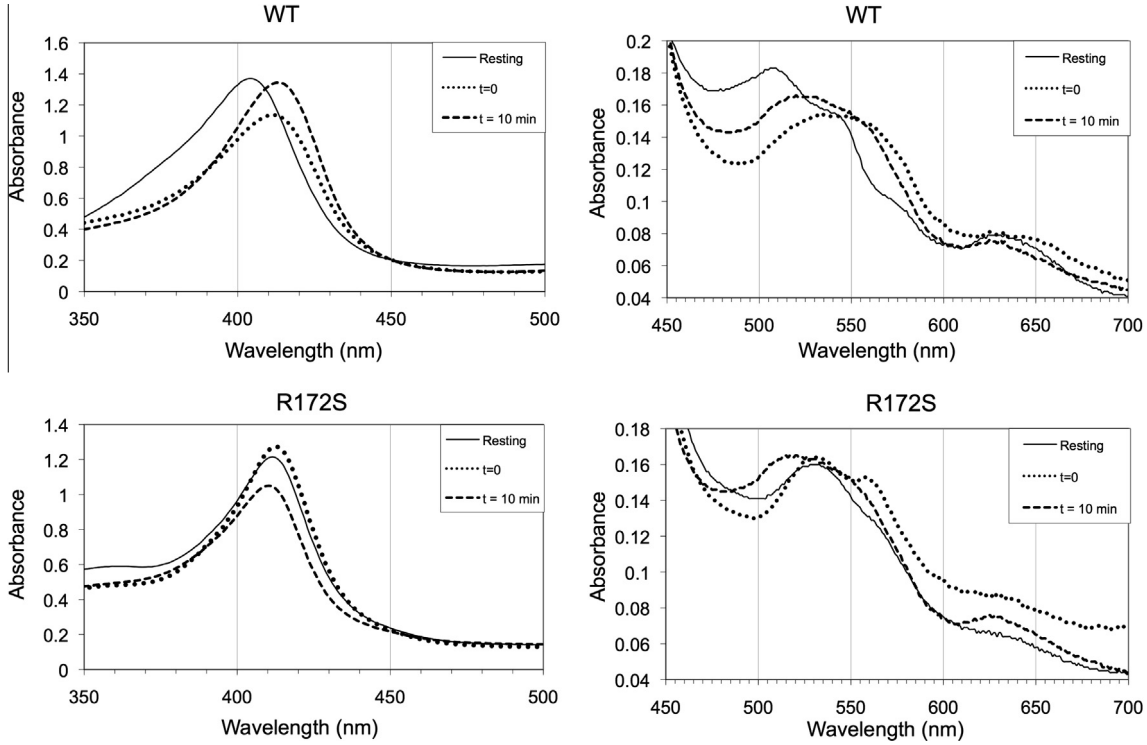

Fig. 4. Spectra of WT and mutant after addition of H_2O_2.

Table 1
Summary of wavelength maxima and shoulders (∗) observed in spectra of resting state, oxidized (1 mol equivalent H_2O_2 added) and reduced state ($Na_2S_2O_4$).

Enzyme – state	Wavelength maxima (nm)
WT – resting	405, 505, 539*, 572*, 637
WT – reduced	433, 509*, 552, 582*
WT – oxidized	412, 520, 550*, 625
R172S – resting	410, 528, 527*, 637
R172S – reduced	424, 527*, 555, 584*
R172S – oxidized	409[a], 520, 550*, 625

2–4 show that the protein is successfully cleaved of its His tag, while lane 5 (same sample as lane 4 but with 5× volume) shows that the purified protein is of real apparent homogeneity.

Comparison of size exclusion chromatography (SEC) with SDS–PAGE results strongly indicates that the native state of rPviAPx is monomeric. The calculated size from the amino acid sequence for the His-tagged protein is 29.5 kDa (calculated using ProtParam from ExPASy) (Wilkins et al., 1999). The His-tagged protein has a size of approximately 26–27 kDa on the SDS–PAGE gel (Fig. 2). The chromatogram for the rPviAPx indicates one major species of 35 kDa with a minor species of 46 kDa. The major species is most likely the monomeric form, since it is relatively close to monomeric sizes determined from the denaturing gel (26 kDa) and the ProtParam calculation (29.5 kDa). The minor species of larger size is most likely an unfavored dimeric form of the protein. Pea and soybean cytosolic APx purified from plant sources are also reported to be homodimeric (Dalton et al., 1987; Mittler and Zilinskas, 1991). However, there is a report of a purified APx from *Zea mays* that was determined to be a 28 kDa momomeric protein via SEC (Koshiba, 1993). From the crystal structure of the recombinant pea APx (rpAPx), it was observed that there are seven residues involved in eight salt-bridge contacts. After aligning the amino acid sequence of rPviAPx to that of rpAPx, it was discovered that six of the seven residues responsible for dimerization are identical. The seventh residue is Asp in Pea but is Lys in rPviAPx. This single amino acid difference would result in a repulsive charge interaction is likely the cause of the loss of dimeric association for rPviAPx. Further inspection of the gene database allowed us to identify a gene for cytosolic APx for Zea mays (NP_001152249.1) that also has this same amino acid difference.

Spectra were collected for WT and mutant in resting, reduced and oxidized states. The reduced state spectra obtained from sodium dithionite reduced WT and mutant are shown in Fig. 3. In the Søret region (Fig, 3A), the WT protein had a resting peak maximum at 405 nm whereas the mutant was at 410 nm. When both proteins were reduced, the Søret peak shifted to 433 nm and 424 nm, respectively. In the 550 nm region of the spectra (Fig. 3B), significant differences between the WT and mutant enzyme spectra were observed. However, in an oxidized state generated by addition of H_2O_2, differences are less pronounced (Fig. 4). Of interest, in the oxidized state for the mutant there was a decrease in the intensity of the peak at 411 nm, and a red-shift was not observed, as compared to the WT enzyme (Fig. 4). Taken together, the spectra of the mutant suggest little spectral change in terms of wavelength in transitioning from a resting to an oxidized state. In contrast, the spectra of the WT showed distinct shifts of 405–412 nm and 505–520 nm. These data suggest that the R172S mutant is shifted from the resting state toward the oxidized state prior to addition of H_2O_2 (Table 1).

2.3. Enzyme activity

The activity of both WT and mutant enzyme was tested using ascorbate and various aromatic substrates. As expected, high activity was observed with ascorbate for the WT enzyme, but very little activity with the mutant. Since APx has been observed to display non-Michaelis–Menten kinetics (Lad et al., 2002), the kinetic constants, K^n (becomes K_m when $n = 1$) and k_{cat} was determined by using the solver function in Excel to find the best-fit parameters for the Hill equation (Eq. (5)). Specifically, solver minimized the root mean square deviation between our data and values

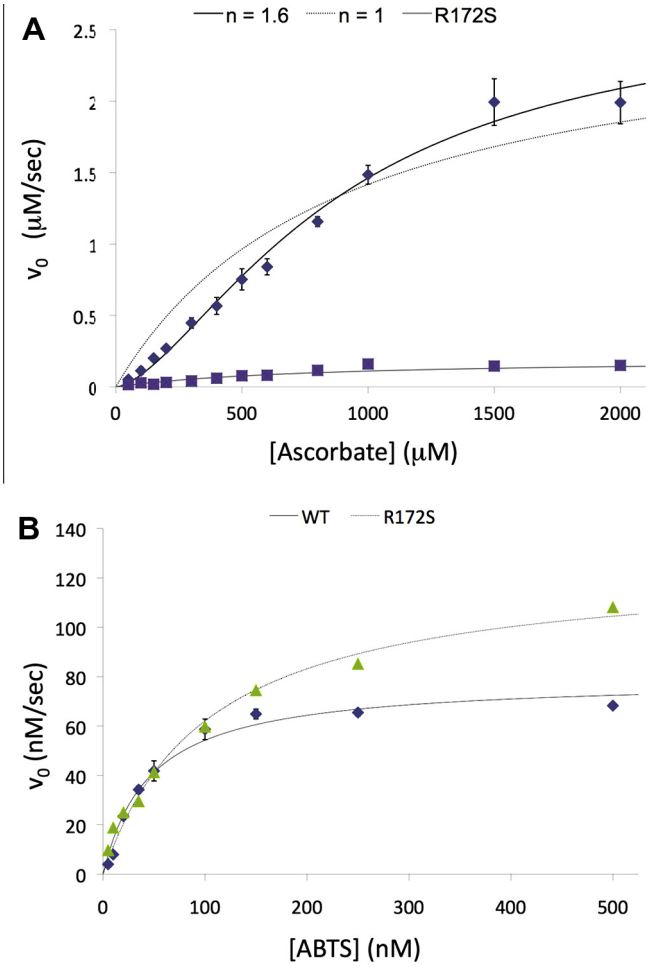

Fig. 5. Enzyme kinetics plots. (A) Plot of Hill equation fit to ascorbate assay data for WT (solid line, diamonds). Dashed line indicates the curve where $n = 1$. Mutant data is plotted with line (gray line, squares) that corresponds to $K^n = 800$ μM and kcat = 14 μM/s, $n = 1$. B) Plots of ABTS activity for WT (solid line, diamonds) and mutant (dotted line, triangles).

calculated using the Hill equation (which reduces to the Michaelis–Menten equation when $n = 1$) by changing V_{max}, K and n. Non-Michaelis–Menten kinetics of WT rPviAPx toward ascorbate was observed (Fig. 5B). This corresponds well to what has been reported for recombinant soybean APx, where strong evidence of two ascorbate binding sites is observed and a non-hyperbolic relationship is observed between velocity and substrate concentration (Lad et al., 2002). The kinetic parameters used to find the best fit where $K^n = 804 \pm 168$ μM and $k_{cat} = 161 \pm 43$ μM/s, where $n = 1.6$ and error is 2 SD for a series of three microplate assays. Because of the very low activity of the mutant, it is difficult to measure the kinetic parameters but the data does fit well to a hyperbolic (Michaelis–Menten kinetics) function, although the error bars are quite large.

$$\frac{v}{V_{max}} = \frac{[S]^n}{K^n + [S]^n} \quad (5)$$

Both the WT and mutant enzymes have activity toward the aromatic compound, 2,2′-azino-bis(3-ethylbenzothiazoline-6-sulfonic acid) (ABTS). Fig. 5A shows a plot of the data for both enzymes, where the same enzyme concentration is used but different k_{cat} and K^n values measured. k_{cat} of 0.40 ± 0.022 s^{-1} and K^n of 43.4 ± 4.04 nM ($n = 1$) for WT and a k_{cat} of 0.67 ± 0.093 s^{-1} and K^n of 110 ± 16 nM ($n = 1$) was observed for the mutant enzyme. However, this activity is much lower than the ascorbate activity. This is somewhat consistent with the relative level of ABTS activity versus ascorbate activity in other APxs, where it has been observed to be as low as 3% of the ascorbate activity (Dalton et al., 1996; Sajitha Rajan and Murugan, 2010). Although, the activity appears to be different between the WT and mutant, the difference is not very large and the mutation does not appear to have a significant effect on ABTS activity compared to WT.

Initial attempts to develop microplate assays for guaiacol and pyrogallol proved to be difficult. Progess curves for each substrate where the substrate concentration was held constant, but the concentration of enzyme was varied indicated that the enzyme is inactivated by the oxidized guaiacol and pyrogallol products. Progress curves for guaiacol, pyrogallol and ABTS (data not shown) indicated that only ABTS did not inactivate the enzyme. The reasons for inactivation arenot clear given that other APxs do not show this behavior. However, it is proposed that it may be due to some sort of covalent modification of the enzyme due to a reaction with the oxidized aromatic radical.

2.4. Structural modeling

The structural model developed from rGmAPx (soybean) using the ascorbate bound structure (PDB ID: 1OAF) gives a good picture of the location of a key active site amino acid, R172 (Fig. 6). From this model, the S172 side-chain of the mutant would be right on the heme corner between the γ and δ sides. If the aromatic binding site is indeed on the δ side of the heme, this would allow the serine side chain to have possible interaction with it. However, it clearly would be unable to interact with the ascorbate binding site in same way as the WT arginine. As a result, the predicted activity with ascorbate would be significantly impacted. The observation of this impact on the actual expressed mutant indicates that our homology model for rPviAPx is useful to make structure/function predictions. Also, unlike a previously tested R172A mutant (Macdonald et al., 2006), the serine residue is still polar and able to hydrogen bond with a heme proprionate group. The R172A mutant had a slightly reduced activity toward the aromatic substrate guaiacol whereas our R172S had a small increase in activity toward ABTS. Admittedly, this is not strong evidence of an influence on aromatic activity but the relatively small impact on aromatic activity fits with what is predicted from the homology model.

3. Conclusions

Overall, our data would suggest that switchgrass cytosolic PviAPx1 has structural and functional characteristics similar to those that have been studied crystallographically (rGmAPx and rPsAPx). The activity toward ascorbate and ABTS are also similar. rPviAPx does differ in that it appears to function as a monomer versus the homodimeric association of these other APxs previously reported. Yet it still displays non-Michaelis–Menten kinetics toward ascorbate. The R172S mutant indicated that ascorbate binding could be abolished without impairing peroxidase activity against other aromatic substances. This is not surprising given the strong structural evidence previously discussed for a separate aromatic binding site (see Section 1). The change made to generate the mutant was targeted to the proposed ascorbate binding site and is far enough away from the aromatic binding site that it would not likely have any influence on activity toward aromatic substrates. It will be interesting to determine if the mutant protein can still play a role in antioxidant defense in plant cells under conditions of ascorbate limitations.

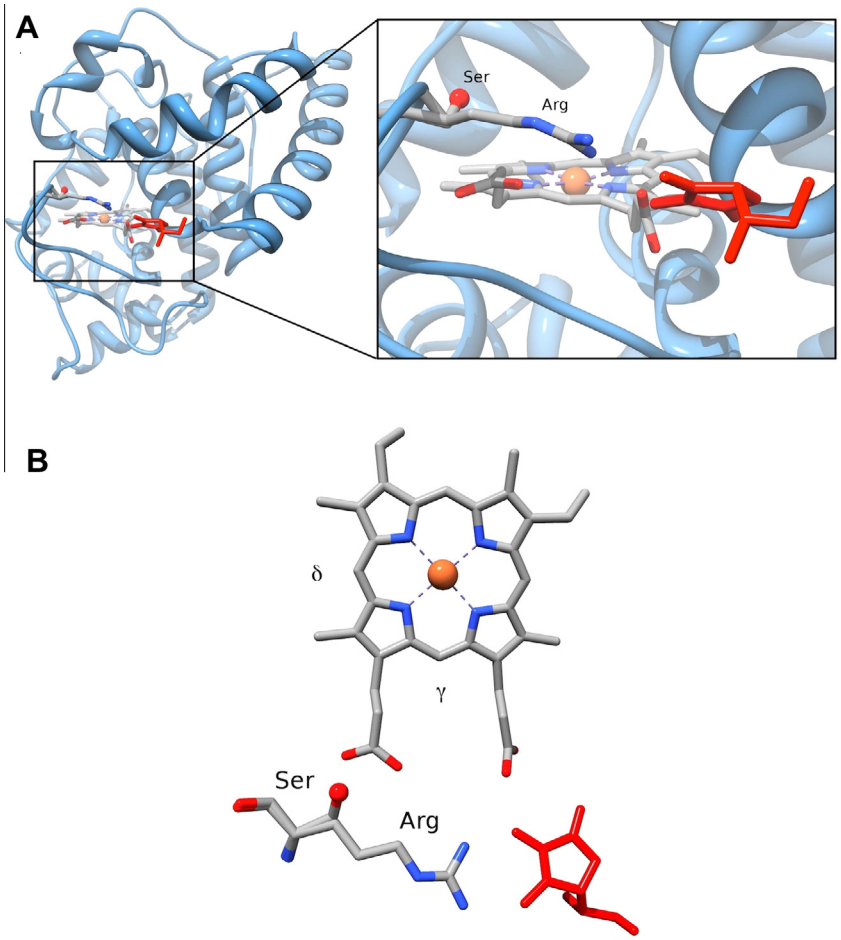

Fig. 6. Homology model for rPviAPx with WT (R172) and mutant (S172) side chains shown relative to heme (based on PDB ID: 1OAF). (A) Side-view of ascorbate binding site with Arg and Ser side chains labeled. (B) Top view of heme showing relative position of Arg and Ser side chains. Ascorbate is shown in red stick representation. (For interpretation of the references to color in this figure legend, the reader is referred to the web version of this article.)

4. Experimental

4.1. Cloning

The open coding frame for a major cytosolic ascorbate peroxidase (rPviAPx; www.phytozome.org, Pavirv00022559m.g) was obtained from a cDNA library prepared from switchgrass callus tissue. The gene was fully sequenced and then cloned out of the library vector, pSPORT1 (Invtrogen). Degenerate PCR primers were used which added restriction enzyme sites to facilitate cloning and expression studies (NdeI (CATATG) to 5′-end and a EcoRI (GAATTC) at the 3′-end. Following sequence verification, the construct was cloned into the pET28a + plasmid (Invitrogen), behind a thrombin cleavable 6X-His tag to the N-terminal end. DNA sequencing was used to verify insertion frame and sequence integrity.

4.2. Homology modeling

Since there is no experimentally derived structural model currently available for rPiAPx, a homology model for the wild type enzyme was developed from the structure of recombinant soybean APx with ascorbate bound (PDB Id: 1OAF, Sharp et al., 2003) using UCSF Chimera (Pettersen et al., 2004) and Modeller (Sali and Blundell, 1993). This model was used to visualize the location of a key active site residue (R172) that interacts with ascorbate. An additional model was generated of a proposed single site APx mutant (R172S) to give a visual perspective of the size difference of the mutation and its location relative to the heme and ascorbate. All molecular images were generated from within Chimera using POV-Ray (Persistence of Vision Pty. Ltd. (2004) Persistence of Vision Raytracer (Version 3.6) retrieved from http://www.povray.org/download/).

4.3. Site-directed mutagenesis

Using pET28a.rPviAPx, site-directed mutagenesis was performed using mutant primers designed via the GeneTailor kit method (Invitrogen) that substituted the Arg_{172} codon (CGA) with a Ser codon (TCA). Platinum® Taq DNA Polymerase High Fidelity (Invitrogen) was used with a protocol that had a 1 min, 56 °C annealing step and a 9 min, 70 °C elongation step. The R172S mutant was verified via DNA sequencing.

4.4. Expression and purification

For protein expression pET28a.rPviAPx was transformed into BL21(DE3) cells. Transformants were fully re-sequenced for rPviAPx and stored at −80 °C as glycerol freezer stocks. These freezer stock were used to start overnight cultures with kanamycin (30 mg/L) which were then used to start expression cultures of 500 mL of 2× YT media in 1 L Erlenmeyer flasks containing kanamycin and 0.5 mM 5-aminolevulinic acid (Research Products International). The expression cultures were incubated at 31 °C with shaking at 150 rpm for 24 h. These cultures were then induced at 0.5 mM IPTG and incubated at 37 °C with shaking at 250 rpm for

6 h. Cells were harvested via centrifugation at which point the cell pellet was observed to have a dark brownish-red color. Pellet was resuspended in lysis buffer (50 mM $NaPO_4$, 500 mM NaCl, 10 mM imidazole, pH 8) to a concentration of 5 mL/g pellet and transfered to metal beaker. Fastbreak solution (Pierce) was added to beaker and solution was shaken at 4 °C for approximately 10 min. This generated very viscous cell lysate which was sonicated with an 11 mm tip using a Sonic Dismembrator – Model 500 (Fisher) until solution was non-viscous. The lysate was then centrifuged at 34,000*g* for 30 min which generated a very red cleared lysate and a fairly small white pellet with a small amount of red. The cleared lysate was filtered prior to purification using 5 mL FastFlow Ni–NTA columns (GE Healthcare), which had been freshly regenerated prior to use. Bound protein was washed first with lysis buffer until the A_{280} came back to baseline. It was then washed with ten column volumes of wash buffer (50 mM $NaPO_4$, 500 mM NaCl, 25 mM imidazole, pH 8). Finally, the protein was eluted with elution buffer (50 mM $NaPO_4$, 500 mM NaCl, 250 mM imidazole, pH 8). Eluted protein was desalted using a series of 5 × 5 mL HiTrap desalting columns (GE Healthcare) into PBS (1×). The desalted protein was treated with thrombin at 1 U/mg protein where protein concentration was calculated from E_{280} (1.11 mL mg^{-1} cm^{-1}, 32.2 mM^{-1} cm^{-1}), which has been measured from highly purified rPviAPx. The cleaved rPviAPx was then passed across a column pre-equilibrated with 50 mM KPO_4 (pH 7) where uncleaved protein was observed to bind to column. The collected protein was very pure as evidenced by an Rz (A_{405}/A_{280}) value of 2.25 and SDS–PAGE (Fig. 2).

4.5. Spectoscopic characterization

Samples of WT and R172S were analyzed spectroscopically using Gen5 software and a Biotek Synergy2 Microplate Reader. Compound I was generated by addition of a molar equivalent of H_2O_2. The reduced forms of the enzymes were generated using $Na_2S_2O_4$ at 0.4 mg/mL.

4.6. Size exclusion chromatography

Size exclusion high performance liquid chromatography (SE-HPLC) was performed to determine the size of the APx using a 300 mm × 4.6 mm analytical SE-HPLC column (Alltech Prosphere SEC 250HR 4 μm 250A) on a HPLC system. A 50 mM Tris–HCl, 100 mM KCl (pH 7) buffer was used for isocratic runs with a flow rate was of 0.35 mL/min. Gel filtration molecular weight markers from Sigma were used to generate a standard curve for native size determination of rPviAPx.

4.7. Enzymatic characterization

The WT and R172S APX were characterized for activity toward ascorbate (E_{290} = 2.8 mM^{-1} cm^{-1}), ABTS (E_{405} = 18.6 mM^{-1} cm^{-1}), guaiacol (E_{470} = 26.6 mM^{-1} cm^{-1}) and pyrogallol (E_{430} = 2.47 mM^{-1} cm^{-1}). Activity characterization was performed using Gen5 software and a Biotek Synergy2 Microplate Reader. For ascorbate, assays were run with 15 nM APx and a range of ascorbate concentrations from 50 to 2000 mM in 50 mM KPO_4 (pH 7). For ABTS, assays were run with 200 nM APx with ABTS concentration going from 5 to 500 mM in 50 mM KPO_4. Enzyme and substrate were combined and added to plate in 100 mL volumes. The reaction was initiated by the addition of 100 mL of 3 mM H_2O_2 giving a final H_2O_2 of 1.5 mM. Background oxidation was measured by combining substrate and H_2O_2 without APx. No assays for guaiacol and pyrogallol were able to be carried out due to enzyme inactivation.

4.8. Bioinformatics

The PviAPx cDNA sequence was translated and used to identify the corresponding gene in the switchgrass genome (www.phytozome.org, switchgrass draft 0.0). The protein sequence was identical to the gene model Pavirv00022559m.g. Other related switchgrass ascobrate peroxidases were identified in the genome, and PviAPx protein sequence was used to identify the best homologs in maize (Zm1), sorghum (Sb1), rice (Os1), pea (Ps1), soybean (Gm1) and Arabidopsis (At1) by BLAST (Altschul et al., 1990). A limited phylogenetic analysis was performed using the Phylogeny.fr server (Dereeper et al., 2010, 2008) using the above protein sequences and default values provided within the program for this analysis to generate a phlylogram using maximal likelihood. Relative expression of cytosolic APx was performed using publically available datasets that have reported transcript abundances in different switchgrass tissues to gauge the expression profiles of select switchgrass cytosolic ascorbate peroxidases. Transcript abundance values were normalized based on total numbers of transcripts within each dataset to allow comparisons between each experiment. These values are an approximate representation and not an absolute value.

Acknowledgements

We thank Nathan Palmer for technical assistance. This work was supported in part by the USDA-ARS CRIS project 5440-21000-030-00D , and by The Office of Science (BER), U. S. Department of Energy Grant Number DE-AI02-09ER64829. The US Department of Agriculture, Agricultural Research Service, is an equal opportunity/affirmative action employer and all agency services are available without discrimination. Mention of commercial products and organizations in this manuscript is solely to provide specific information. It does not constitute endorsement by USDA-ARS over other products and organizations not mentioned. This work was also supported in part by funding provided by the UNK Office of Graduate Studies and Research/Research Services Council.

Some of the equipment used in this project was purchased from NIH grant number 1 P20 RR16469 from the INBRE Program of the National Center for Research Resources.

References

Altschul, S.F., Gish, W., Miller, W., Myers, E.W., Lipman, D.J., 1990. Basic local alignment search tool. J. Mol. Biol. 215, 403–410.

Alvarez, M.E., Lamb, C., varez and Lamb 1997. Oxidative Burst-mediated Defense Responses in Plant Disease Resistance. Cold Spring Harbor Monograph Archive, North America 34, 815–839.

Bowler, C., Montagu, M.V., Inze, D., 1992. Superoxide dismutase and stress tolerance. Ann. Rev. Plant Physiol. Plant Mol. Biol. 43, 83–116.

Cheek, J., Mandelman, D., Poulos, T.L., Dawson, J.H., 1999. A study of the K(+)-site mutant of ascorbate peroxidase: mutations of protein residues on the proximal side of the heme cause changes in iron ligation on the distal side. J. Biol. Inorg. Chem. 4, 64–72.

Chen, Z., Young, T.E., Ling, J., Chang, S.C., Gallie, D.R., 2003. Increasing vitamin C content of plants through enhanced ascorbate recycling. Proc. Nat. Acad. Sci. U.S.A. 100, 3525–3530.

Dalton, D.A., Diaz del Castillo, L., Kahn, M.L., Joyner, S.L., Chatfield, J.M., 1996. Heterologous expression and characterization of soybean cytosolic ascorbate peroxidase. Arch. Biochem. Biophys. 328, 1–8.

Dalton, D.A., Hanus, F.J., Russell, S.A., Evans, H.J., 1987. Purification, properties, and distribution of ascorbate peroxidase in legume root nodules. Plant Physiol. 83, 789–794.

Dereeper, A., Audic, S., Claverie, J.M., Blanc, G., 2010. BLAST-EXPLORER helps you building datasets for phylogenetic analysis. BMC Evol. Biol. 10, 8.

Dereeper, A., Guignon, V., Blanc, G., Audic, S., Buffet, S., Chevenet, F., Dufayard, J.F., Guindon, S., Lefort, V., Lescot, M., Claverie, J.M., Gascuel, O., 2008. Phylogeny.fr: robust phylogenetic analysis for the non-specialist. Nucleic Acids Res. 36, W465–W469.

Dunford, H.B., 1999. Heme Peroxidases. John Wiley, New York.

Groden, D., Beck, E., 1979. H2O2 destruction by ascorbate-dependent systems from chloroplasts. Biochim. Biophys. Acta 546, 426–435.

Ishikawa, T., Shigeoka, S., 2008. Recent advances in ascorbate biosynthesis and the physiological significance of ascorbate peroxidase in photosynthesizing organisms. Biosci. Biotechnol. Biochem. 72, 1143–1154.
Kelly, G.J., Latzko, E., 1979. Soluble ascorbate peroxidase: detection in plants and use in vitamim C estimation. Naturwissenschaften 66, 617–619.
Koshiba, T., 1993. Cytosolic ascorbate peroxidase in seedlings and leaves of maize (*Zea mays*). Plant Cell Physiol. 34, 713–721.
Lad, L., Mewies, M., Raven, E.L., 2002. Substrate binding and catalytic mechanism in ascorbate peroxidase: evidence for two ascorbate binding sites. Biochemistry 41, 13774–13781.
Macdonald, I.K., Badyal, S.K., Ghamsari, L., Moody, P.C., Raven, E.L., 2006. Interaction of ascorbate peroxidase with substrates: a mechanistic and structural analysis. Biochemistry 45, 7808–7817.
Martell, J.D., Deerinck, T.J., Sancak, Y., Poulos, T.L., Mootha, V.K., Sosinsky, G.E., Ellisman, M.H., Ting, A.Y., 2012. Engineered ascorbate peroxidase as a genetically encoded reporter for electron microscopy. Nat. Biotechnol. 30, 1143–1148.
Metcalfe, C., Macdonald, I.K., Murphy, E.J., Brown, K.A., Raven, E.L., Moody, P.C., 2008. The tuberculosis prodrug isoniazid bound to activating peroxidases. J. Biol. Chem. 283, 6193–6200.
Mittler, R., Zilinskas, B.A., 1991. Purification and characterization of pea cytosolic ascorbate peroxidase. Plant Physiol. 97, 962–968.
Noctor, G., Foyer, C.H., 1998. Ascorbate and glutathione: keeping active oxygen under control. Annu. Rev. Plant Physiol. Plant Mol. Biol. 49, 249–279.
Patterson, W.R., Poulos, T.L., 1995. Crystal structure of recombinant pea cytosolic ascorbate peroxidase. Biochemistry 34, 4331–4341.
Pettersen, E.F., Goddard, T.D., Huang, C.C., Couch, G.S., Greenblatt, D.M., Meng, E.C., Ferrin, T.E., 2004. UCSF Chimera – a visualization system for exploratory research and analysis. J. Comput. Chem. 25, 1605–1612.
Raven, E.L., 2003. Understanding functional diversity and substrate specificity in haem peroxidases: what can we learn from ascorbate peroxidase? Nat. Prod. Rep. 20, 367–381.
Raven, E.L., Lad, L., Sharp, K.H., Mewies, M., Moody, P.C., 2004. Defining substrate specificity and catalytic mechanism in ascorbate peroxidase. Biochem. Soc. Symp., 27–38.
Sajitha Rajan, S., Murugan, K., 2010. Purification and kinetic characterization of the liverwort *Pallavicinia lyelli* (Hook.) S. Gray. cytosolic ascorbate peroxidase. Plant Physiol. Biochem. 48, 758–763.
Sali, A., Blundell, T.L., 1993. Comparative protein modelling by satisfaction of spatial restraints. J. Mol. Biol. 234, 779–815.
Sarath, G., Mitchell, R.B., Sattler, S.E., Funnell, D., Pedersen, J.F., Graybosch, R.A., Vogel, K.P., 2008. Opportunities and roadblocks in utilizing forages and small grains for liquid fuels. J. Ind. Microbiol. Biotechnol. 35, 343–354.
Sharp, K.H., Mewies, M., Moody, P.C., Raven, E.L., 2003. Crystal structure of the ascorbate peroxidase-ascorbate complex. Nat. Struct. Biol. 10, 303–307.
Sharp, K.H., Moody, P.C., Brown, K.A., Raven, E.L., 2004. Crystal structure of the ascorbate peroxidase–salicylhydroxamic acid complex. Biochemistry 43, 8644–8651.
Shigeoka, S., Ishikawa, T., Tamoi, M., Miyagawa, Y., Takeda, T., Yabuta, Y., Yoshimura, K., 2002. Regulation and function of ascorbate peroxidase isoenzymes. J. Exp. Bot. 53, 1305–1319.
Teixeira, F.K., Menezes-Benavente, L., Margis, R., Margis-Pinheiro, M., 2004. Analysis of the molecular evolutionary history of the ascorbate peroxidase gene family: inferences from the rice genome. J. Mol. Evol. 59, 761–770.
Wilkins, M.R., Gasteiger, E., Bairoch, A., Sanchez, J.C., Williams, K.L., Appel, R.D., Hochstrasser, D.F., 1999. Protein identification and analysis tools in the ExPASy server. Methods Mol. Biol. 112, 531–552.